Recombinant cathepsin S propeptide attenuates cell invasion by inhibition of cathepsin L–like proteases in tumor microenvironment

Roberta E. Burden,[1] Philip Snoddy,[3] Richard J. Buick,[3] James A. Johnston,[2] Brian Walker,[1] and Christopher J. Scott[1]

[1]School of Pharmacy and [2]Centre for Cancer Research and Cell Biology, Queen's University of Belfast; and [3]Fusion Antibodies Ltd., Belfast, Northern Ireland

Abstract

Human cathepsin L along with cathepsin S, K, and V are collectively known as cathepsin L–like proteases due to their high homology. The overexpression and aberrant activity of each of these proteases has been implicated in tumorigenesis. These proteases contain propeptide domains that can potently inhibit both their cognate protease and other proteases within the cathepsin L–like subfamily. In this investigation, we have produced the cathepsin S propeptide recombinantly and have shown that it is a potent inhibitor of the peptidolytic, elastinolytic, and gelatinolytic activities of the cathepsin L–like proteases. In addition, we show that this peptide is capable of significantly attenuating tumor cell invasion in a panel of human cancer cell lines. Furthermore, fusion of an IgG Fc-domain to the COOH terminus of the propeptide resulted in a chimeric protein with significantly enhanced ability to block tumor cell invasion. This Fc fusion protein exhibited enhanced stability in cell-based assays in comparison with the unmodified propeptide species. This approach for the combined inhibition of the cathepsin L–like proteases may prove useful for the further study in cancer and other conditions where their aberrant activity has been implicated. Furthermore, this strategy for simultaneous inhibition of multiple cysteine cathepsins may represent the basis for novel therapeutics to attenuate tumorigenesis. [Mol Cancer Ther 2008;7(3):538–47]

Received 8/3/07; revised 11/8/07; accepted 1/21/08.

Grant support: Department of Education and Learning, Northern Ireland and Fusion Antibodies Ltd. Co-Operative Awards in Science and Technology Studentship (R.E. Burden).

The costs of publication of this article were defrayed in part by the payment of page charges. This article must therefore be hereby marked *advertisement* in accordance with 18 U.S.C. Section 1734 solely to indicate this fact.

Requests for reprints: Christopher J. Scott, School of Pharmacy, Queen's University of Belfast, 97 Lisburn Road, Belfast BT9 7BL, Northern Ireland. Phone: 440-2890972350. E-mail: c.scott@qub.ac.uk

doi:10.1158/1535-7163.MCT-07-0528

Introduction

Cathepsin L–like proteases are closely related members of the C1 family of papain-like cysteine proteases and include cathepsins L, K, S, and V (1). Normally localized in the lysosomes, specific roles for these proteases have been established, including their contribution in the processes of antigen presentation (2, 3), bone resorption (4), and extracellular matrix remodeling (5, 6).

One of the main mechanisms to regulate the activity of the cysteine cathepsins is their synthesis as inactive zymogens. The NH_2-terminal propeptide domain of the cathepsin L–like proteases is an inhibitor of the active enzyme in its latent form, which is then removed on its activation (7, 8). Using purified proteases in peptidolytic assays, the ability of the propeptide to act as reversible inhibitors of their cognate protease has been shown (9, 10). Moreover, due to the conserved homology in their sequence, each propeptide can inhibit other cathepsins within this distinct subfamily of cathepsin L–like proteases with low nanomolar potencies (8–12).

In addition to their normal physiologic roles, the aberrant activity of cathepsin L–like proteases has been shown to promote tumorigenesis (13–15). Evidence showing the overexpression, secretion, and inappropriate activity of these proteases suggests that they contribute to the hydrolysis of extracellular matrix directly through their ability to degrade components such as laminin, fibronectin, and collagen (16, 17), thus facilitating the invasive nature of the tumor cells through their microenvironment.

To collectively examine the role of the extracellular cathepsin L–like proteases in tumor cell invasion, we have generated a recombinant human cathepsin S propeptide (rCatSPP). The inhibitory activity of this rCatSPP was determined by steady-state fluorimetric assays, which revealed its ability to selectively inhibit the cathepsin L–like subfamily of lysosomal cysteine proteases. Further demonstration of the ability of the rCatSPP to act as an inhibitor of this subfamily was furnished in a series of *in vitro* tumor cell invasion assays. Manipulation of the rCatSPP to contain a COOH-terminal IgG Fc-domain enhanced the stability of the recombinant protein and its application to invasion assays showed a significant increase in effectiveness in comparison to the original rCatSPP species.

Materials and Methods

Cell Culture

The U251mg, MDA-MB-231, PC3, and HCT116 cell lines were obtained from the American Type Culture Collection. U251mg and MDA-MB-231 cells were cultured in DMEM,

whereas PC3 and HCT116 cell lines were cultured using RPMI 1640 and McCoy's 5A medium, respectively, supplemented with 10% FCS and 2% L-glutamine. All cells were maintained in a humidified environment containing 5% CO_2 at 37°C.

Cloning of rCatSPP and rCatSPP-Fc

The open reading frame for CatSPP (residues 17-113 of human cathepsin S) was amplified from a human spleen cDNA library (Origene) using primers CatSPP forward (5′-TTTTTT*GGATCC*CAGTTGCATAAAGATCCTAC) and CatSPP reverse (5′-TTTTTT*GTCGAC*CCGATTAGGGTTTGA) containing *Bam*HI and *Sal*I restriction sites, respectively (as italicized). The expected band of 330 bp was visualized by agarose electrophoresis and subsequently cloned into the pQE-30 bacterial expression vector (Qiagen), incorporating an NH_2-terminal hexahistidine tag [$(His)_6$ tag] to enable downstream purification. Positive clones were identified by colony PCR and sequence aligned to accession no. M90696. A single verified clone was used in all subsequent experiments. Similarly, the same PCR fragment pertaining to CatSPP was inserted into a modified pRSET vector (Invitrogen) containing the open reading frame for murine IgG_{2b} Fc CH2 and CH3 domains. Expression from this ligated vector resulted in the generation of the CatSPP with an NH_2-terminal $(His)_6$ tag as before and including the COOH-terminal murine Fc-domain. Positive clones were verified, as before, by DNA sequencing.

Protein Expression and Purification of rCatSPP and rCatSPP-Fc

A positive clone was transformed into TOP10F′ *Escherichia coli* cells and cultured until reaching mid-log phase (A_{550} = 0.5; 37°C). Expression of rCatSPP was induced by the addition of IPTG (1 mmol/L) and propagated for a further 4 h before harvesting. Cell pellets were resuspended and lysed in 50 mmol/L NaH_2PO_4 (pH 8.0) containing 8 mol/L urea, 300 mmol/L NaCl, and 10 mmol/L imidazole. The crude denatured lysate was clarified by centrifugation (10,000 × *g*, 60 min at 4°C) before application to an immobilized metal affinity chromatography (IMAC) column charged with Ni^{2+} ions (HiTrap 1 mL column; GE Healthcare). Nonspecifically bound material was washed from the column using 50 mmol/L NaH_2PO_4 (pH 8.0) containing 8 mol/L urea, 300 mmol/L NaCl, and 20 mmol/L imidazole followed by on-column refolding by reduction of the urea from 8 to 0 mol/L over 200 column volumes. Refolded column-bound material was washed with a further 20 column volumes of 50 mmol/L NaH_2PO_4 (pH 8.0), 300 mmol/L NaCl, and 20 mmol/L imidazole then eluted with 50 mmol/L NaH_2PO_4 (pH 8.0), 300 mmol/L NaCl, and 250 mmol/L imidazole. Protein fractions were collected, desalted into PBS, and analyzed by SDS-PAGE and Western blotting to determine purity and integrity. Concentrations of the rCatSPP were determined using the BCA method (Pierce) and stocks of purified rCatSPP were stored at -20°C before use.

Similarly, expression of the CatSPP-Fc chimera was done using BL21(DE3)pLysS cells, whereby the cells were cultured and recombinant protein was induced again using IPTG at 37°C for 4 h. Cells were harvested and the rCatSPP-Fc protein isolated and purified via its NH_2-terminal $(His)_6$ tag using the same procedure for the rCatSPP described above.

Inhibition of Cathepsin S with rCatSPP

Fluorimetric assays were done in triplicate in 96-well microtitre plates in the presence of 100 mmol/L sodium acetate, 1 mmol/L EDTA, 0.1% Brij, and 1 mmol/L DTT (pH 5.5) using cathepsins S, L, K, V, and B (Calbiochem). Cathepsin S activity was monitored using the fluorogenic substrate carbobenzloxy-L-valinyl-L-valinyl-L-arginylamido-4-methyl coumarin (Cbz-Val-Val-Arg-AMC; 25 μmol/L). Similar assays for cathepsins L, K, and V were done using carbobenzloxy-L-phenylalanyl-L-arginylamido-4-methyl coumarin (Cbz-Phe-Arg-AMC; 5 μmol/L for cathepsin L and 25 μmol/L for cathepsin K and V), whereas assays for cathepsin B were done using carbobenzloxy-L-arginylamido-L-arginylamido-4-methyl coumarin (Cbz-Arg-Arg-AMC; 25 μmol/L) as substrates. Purified rCatSPP or rCatSPP-Fc was added to assays at various concentrations and the resultant fluorescence was measured using a Cytofluor 4000 spectrofluorimeter with excitation at 395 nm and emission at 460 nm wavelengths. Fluorimetric assays using the fluorescently labeled DQ-elastin and DQ-gelatin (Invitrogen) were done as above (100 μg/mL), with excitation and emission wavelengths of 480 and 530 nm, respectively.

The relative level of cathepsin L–like subfamily activity in the human malignant cell lines was also determined by fluorimetric assays. Conditioned medium was retained and cell lysates were prepared using a 100 mmol/L sodium acetate lysis buffer containing 100 mmol/L NaCl and 0.1% Triton X-100. The cell suspension was sonicated to ensure complete cell disruption, and after centrifugation, cell lysates and conditioned medium samples were subjected to BCA analysis to determine protein concentration. The relative levels of cathepsin L–like activity were measured by incubating samples (100 μg/mL) with 0.5 mol/L MES buffer (pH 6.0) containing 2 mmol/L DTT. The substrate Cbz-Val-Val-Arg-AMC (5 μmol/L) was added, and the rate of substrate hydrolysis at 37°C was monitored every 60 s over a period of 60 min.

Reverse Transcription-PCR

RNA was extracted from the mammalian cell lines using the Absolutely RNA RT-PCR Miniprep kit (Stratagene). Reverse transcription-PCR was done using the One-Step RT-PCR kit (Qiagen) under the following conditions: 50°C for 30 min, 95°C for 15 min, and 35 cycles of 94°C for 1 min, 55°C for 90 s, and 72°C for 1 min followed by a final incubation at 72°C for 10 min. Primer sequences for target genes were as follows: cathepsin S forward GGGTACCTC-ATGTGACAAG and reverse TCACTTCTTCACTGGTCATG, cathepsin L forward ATGAATCCTACACTCATCCTTGC and reverse TCACACAGTGGGGTAGCTGGCTGCTG, cathepsin K forward ATGTGGGGGCTCAAGGTTCTGC and reverse TCACATCTTGGGGAAGCTGGCC, cathepsin V forward ATGAATCTTTCGCTCGTCCTGGC and reverse TCACACATTGGGGTAGCTGGC, and actin forward

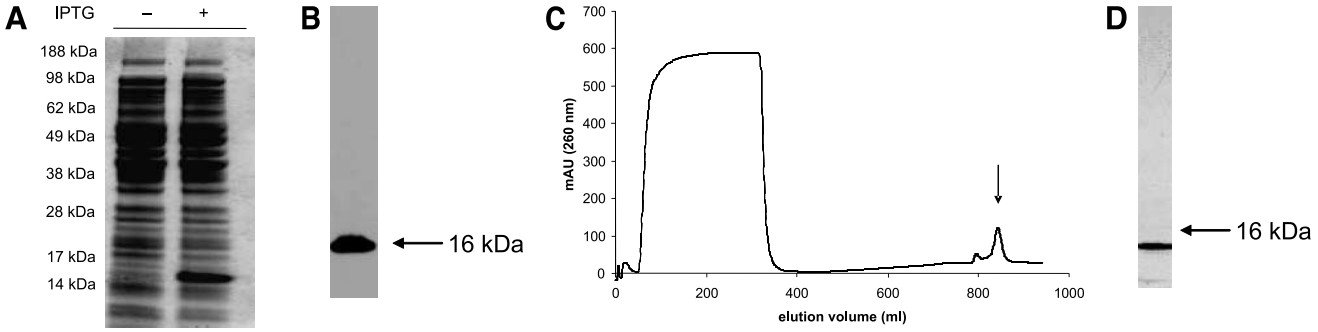

Figure 1. Expression and purification of rCatSPP. The DNA sequence encoding the rCatSPP was cloned into the pQE-30 bacterial vector, allowing the incorporation of a NH_2-terminal $(His)_6$ tag. Expression of the rCatSPP was induced using IPTG. Lysates were taken from an uninduced control and induced *E. coli* cultures and analyzed by SDS-PAGE and confirmed expression and inducibility of the rCatSPP at ~16 kDa (**A**). Lysates were also electrophoresed and transferred to nitrocellulose membrane. Western blotting with an anti-polyhistidine tag antibody was used to confirm expression and presence of the $(His)_6$ tag (**B**). The rCatSPP was purified by IMAC; the first broad peak represents loading of the denatured sample onto the HiTrap column, the second represents elution of nonspecifically bound proteins, and the third (↓) shows elution of the $(His)_6$-tagged rCatSPP (**C**). Eluted fractions from the third peak were analyzed by SDS-PAGE with Coomassie staining to confirm successful purification and to assess purity (**D**).

ATCTGGCACCACACCTTCTACAATGAGCTGCG and reverse CGTCATACTCCTGCTTGCTGATCCACATCTGC.

In vitro Invasion Assays

In vitro invasion assays were done as described previously (18). Briefly, cells were incubated in the presence of predetermined concentrations of rCatSPP, rCatSPP-Fc, or appropriate controls, and invasion plates were incubated at 37°C and 5% CO_2 for 24 h. Noninvaded cells were removed and invaded cells were fixed in Carnoy's fixative for 15 min. After drying, the nuclei of the invaded cells were stained with Hoechst 33258 (50 ng/mL) in PBS for 30 min at room temperature. The chamber insert was washed twice in PBS and mounted in Citifluor, and invaded cells were viewed with a Nikon Eclipse TE300 fluorescent microscope. All assays were done in triplicate and 10 digital images of representative fields from each of the triplicate membranes were taken using a Nikon DXM1200 digital camera at magnification of ×20. Results were analyzed using Lucia GF 4.60 software by Laboratory Imaging. The results were expressed using untreated control cells (0 nmol/L) as 100% cell invasion, and all other readings were expressed as percentage ± SD cell invasion. The Student's *t* test was used to determine the statistical significance of the reduction in invasion observed in the presence of the rCatSPP. To determine EC_{50} values for rCatSPP and rCatSPP-Fc, relative rates of invasion were subjected to nonlinear regression analysis using Prism software.

MTT Cell Viability Assay

Cytotoxicity of the rCatSPP was determined using the MTT cell viability assay. Briefly, cells were seeded at 1×10^4 per well of a 96-well microtiter plate in 200 μL medium. Appropriate concentrations of rCatSPP (200 nmol/L), control protein, or vehicle-only control were added to the cells and incubated at 37°C and 5% CO_2 for 24, 48, and 72 h, respectively. After incubation, conditioned medium was removed and 0.5 mg/mL MTT (200 μL) was added to the wells and incubated for a further 2 h at 37°C and 5% CO_2. The MTT reagent was carefully removed and the insoluble formazan crystals were dissolved in 100 μL/well DMSO. Absorbance was measured at 570 nm and the results were expressed as the percentage cell viability relative to vehicle-only control. All tests were done in quintuplicate.

Stability Assay

To compare the relative stabilities of the rCatSPP and rCatSPP-Fc, 500 nmol/L of each protein were incubated with HCT116 cells and stability of the proteins was evaluated by Western blotting of the cell supernatants over 24 h. Supernatants were resolved by SDS-PAGE using 4% to 12% bis-Tris gels and MOPS running buffer and proteins were subsequently transferred to polyvinylidene difluoride membranes and immunoblotted using an anti-polyhistidine tag horseradish peroxidase–conjugated antibody (1:3,000; Sigma).

Results

Expression and Purification of rCatSPP

To enable the generation of rCatSPP, the DNA sequence encoding the CatSPP (residues 17-113) was amplified and cloned into the bacterial expression vector, enabling the expression of the domain with an NH_2-terminal $(His)_6$ tag at the expected molecular weight of ~16 kDa. Expression of the rCatSPP from TOP10F′ *E. coli* cells was shown to be inducible and regulated by the addition of IPTG through the analysis of cell lysates by SDS-PAGE and Coomassie blue staining (Fig. 1A). The presence of the $(His)_6$ tag was confirmed by immunoblotting with an anti-polyhistidine horseradish peroxidase–conjugated antibody (Fig. 1B). The $(His)_6$-tagged protein was expressed insolubly (data not shown); therefore, after harvesting, cells were lysed and proteins were denatured in 8 mol/L urea phosphate buffer before application to a Ni^{2+}-charged IMAC column. On-column refolding was done by the complete removal of the chaotropic agent over a linear gradient from 8 to 0 mol/L. The column bound material was subsequently eluted using

an imidazole gradient (0-250 mmol/L), resulting in the generation of two elution peaks (Fig. 1C). Analysis of eluted fractions from the second purification peak by SDS-PAGE identified the presence of the purified rCatSPP (Fig. 1D).

Enzyme Inhibition Assays

The inhibitory activity of the refolded rCatSPP was determined initially against recombinant, mature human cathepsin S, employing a steady-state fluorimetric assay. Typical progress curves for the cathepsin S–catalyzed hydrolysis of Cbz-Val-Val-Arg-AMC in the presence of varying concentrations of the rCatSPP are shown in Fig. 2A (*main graph*). These progress curves are indicative of the action of a slow tight-binding reversible inhibitor. The progress curves were subjected to nonlinear regression analysis (19) where the production of fluorescence [P] over time can be represented by the following equation:

$$[P] - v_s t - (v_s - v_0)(1 - exp(-k_{obs} t))/k_{obs} + d \qquad (1)$$

In this equation, v_s is the final steady state rate and v_0 is the initial steady state rate for the formation of product. The term d is a displacement term that represents the concentration of product at $t = 0$. The apparent first-order rate constant k_{obs} is a reflection of the time-dependent nature of the transition between the initial and the steady state rates. Using GraFit software, data points from the progress curves were fitted to Eq. (1) and values of v_s were then determined for each inhibitor concentration employed. These were then used to generate Morrison plots (v_s against [I]; Fig. 2A, *inset*) from which $K_{i\ (observed)}$ was determined. This was then corrected to account for competing substrate, as shown in Eq. (2), giving a true K_i value of 2.5 ± 0.12 nmol/L against cathepsin S.

$$K_i = K_{i(observed)}/(1 + [S]/K_m). \qquad (2)$$

The ability of the rCatSPP to inhibit the peptidolytic activities of recombinant human cathepsins K, L, and V were also determined by fluorimetric assays (Fig. 2B-*D, main graphs*). The final steady-state rates from the resultant progress curves for the inhibition of these proteases with rCatSPP were also calculated and used to generate additional ''Morrison plots'' (Fig. 2B–D, *insets*). The rCatSPP was found to function as a potent inhibitor of each of the cathepsin L–like proteases, exhibiting K_i values of 13.9 ± 2.4 nmol/L, 17.6 ± 1.3 nmol/L, and 4.3 ± 0.6 nmol/L for cathepsins L, K and V, respectively. No discernable inhibitory activity against the more distantly related cathepsin B was observed (data not shown).

The low nanomolar K_i values obtained in this investigation are comparable with those reported previously for the inhibition of the cathepsin L–like proteases by their

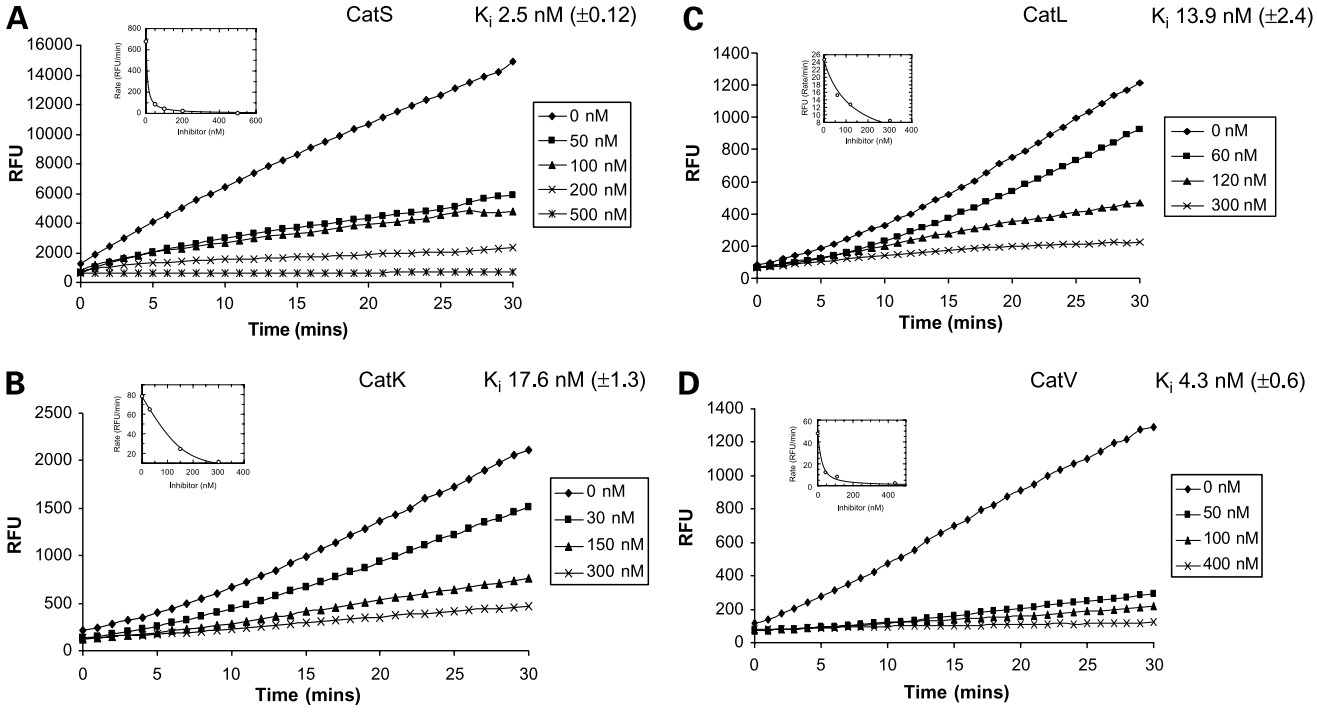

Figure 2. Inhibition of the peptidolytic activity of the cathepsin L–like proteases. Protease activity was assessed by monitoring cleavage of fluorigenic substrates, cathepsin S–mediated cleavage of Cbz-Val-Val-Arg-AMC (**A**), cathepsin K (**B**), cathepsin L (**C**), and cathepsin V cleavage of Cbz-Phe-Arg-AMC (**D**), in the presence of increasing concentrations of rCatSPP. Rates were extrapolated from the progress curves, subjected to nonlinear regression analysis, and fitted to Morrison binding curves to calculate K_i values (*inset*).

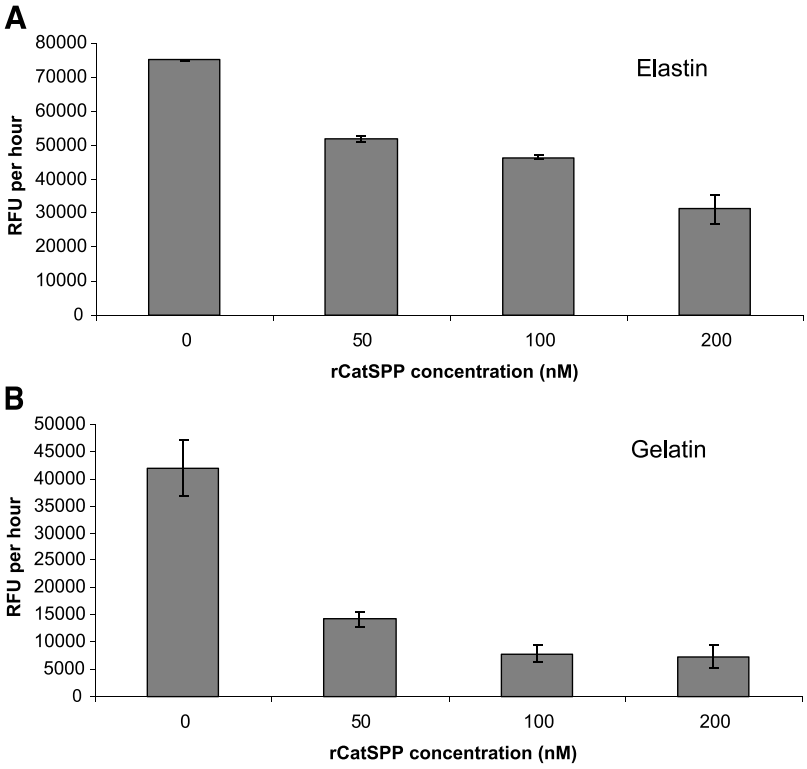

Figure 3. Effect of the rCatSPP on the elastinolytic and gelatinolytic activity of cathepsin S. Fluorimetric assays were done in the presence of the rCatSPP (0-200 nmol/L) to inhibit cathepsin S–mediated cleavage of DQ-elastin (**A**) and DQ-gelatin (**B**; 100 μg/mL).

respective propeptides, but there are some minor differences between the reported values and those determined herein. However, these can be attributed to the differences in the composition of assay buffers used in the present and previous studies. Previously, Guay et al. showed that the replacement of a 50 mmol/L citrate assay buffer by a 50 mmol/L MES buffer led to the total abolition of the inhibition of cathepsins L, S, and K by the rCatKPP (9). In these experiments, the fluorimetric assays were done in a 100 mmol/L sodium acetate buffer (pH 5.5), as has been published previously (20, 21), and is suitable for use with the each of the cathepsin L–like cysteine cathepsins.

rCatSPP Blocks Elastinolytic and Collagenolytic Activities of Cathepsin S

The ability of the rCatSPP to attenuate the elastinolytic and collagenolytic activity of cathepsin S was determined by fluorimetric assays using the fluorescently labeled (BODIPY) elastin and gelatin proteolytic substrates, DQ-elastin and DQ-gelatin. The assays were done using activated cathepsin S in the presence of increasing concentrations rCatSPP. The rCatSPP appears to have the ability to attenuate the cleavage of both DQ-elastin and DQ-gelatin (Fig. 3). A reduction in the ability of cathepsin S to cleave elastin was observed, with 60% reduction is elastinolytic activity observed in the presence of the rCatSPP (200 nmol/L; Fig. 3A). Likewise, a 80% reduction in cathepsin S–mediated collagenolytic activity was also observed in the presence of the rCatSPP (200 nmol/L; Fig. 3B).

Inhibition of Tumor Cell Invasion by the rCatSPP

Next, we investigated if the *in vitro* inhibition of the cathepsin L–like proteases by the rCatSPP would result in blockage of tumor cell invasion. Cell lines representative of different types of invasive malignancy were selected: PC3 (prostate), HCT116 (colorectal), U251mg (astrocytoma), and MDA-MB-231 (breast). The presence of the different cathepsin L–like subfamily proteases within the panel of human malignant cell lines was verified by reverse transcription-PCR (Fig. 4A). The presence of mRNA for each protease was clearly evident in all four cell lines, with the exception of cathepsin V. Cathepsin V expression was almost negligible in the MDA-MB-231 breast carcinoma cell line. In addition, the activity of the cathepsin L–like proteases was determined by fluorimetric assay in the conditioned medium and cell lysates (Fig. 4B), further showing that these proteases are expressed in and secreted from these tumor cell lines.

The human malignant cell lines were examined in a series of *in vitro* invasion assays to ascertain the extent to which the secreted cathepsin L–like proteases promote tumor cell invasion through their inhibition by the rCatSPP. Tumor cells were incubated with the rCatSPP (0-200 nmol/L) for 24 h to determine the relative rates of invasion through the Matrigel-coated Transwells. As controls, an unrelated recombinant protein produced from the same bacterial expression vector (200 nmol/L) and a vehicle-only buffer control were also incubated with the cells under identical conditions. The rCatSPP was found to attenuate the rate of tumor cell invasion in a dose-dependent fashion in each of

the cell lines examined (Fig. 4C). The greatest attenuation of invasion was observed with the HCT116 colorectal carcinoma cells, with a 58% reduction in invasion observed in the presence of 200 nmol/L of the rCatSPP ($P < 0.0001$; Fig. 4C, *first panel*). A significant inhibition of tumor cell invasion was also observed for the other cell lines, with a 48%, 47%, and 35% reduction in invasion observed for PC3, MDA-MB-231, and U251mg cells in the presence of 200 nmol/L of the rCatSPP ($P < 0.01$, <0.0001, and <0.001, respectively; Fig. 4C, *remaining panels*).

To confirm that the observed reduction in tumor invasion was not simply due to antiproliferative or cytotoxic effects of the rCatSPP, MTT assays were done. For example, HCT116 cells were incubated with the rCatSPP (200 nmol/L), control protein (200 nmol/L), or vehicle-only control for 24, 48, and 72 h and the number of viable cells was counted/compared for each treatment. No significant effects on cell viability by the rCatSPP or control protein were detected; therefore, the anti-invasive effects observed were solely due to the inhibition of the cathepsin L–like proteases, which facilitate tumor invasion (Fig. 4D).

Expression and Purification of rCatSPP-Fc

Based on the significant anti-invasive effects observed with the rCatSPP, we asked if the effects could be improved

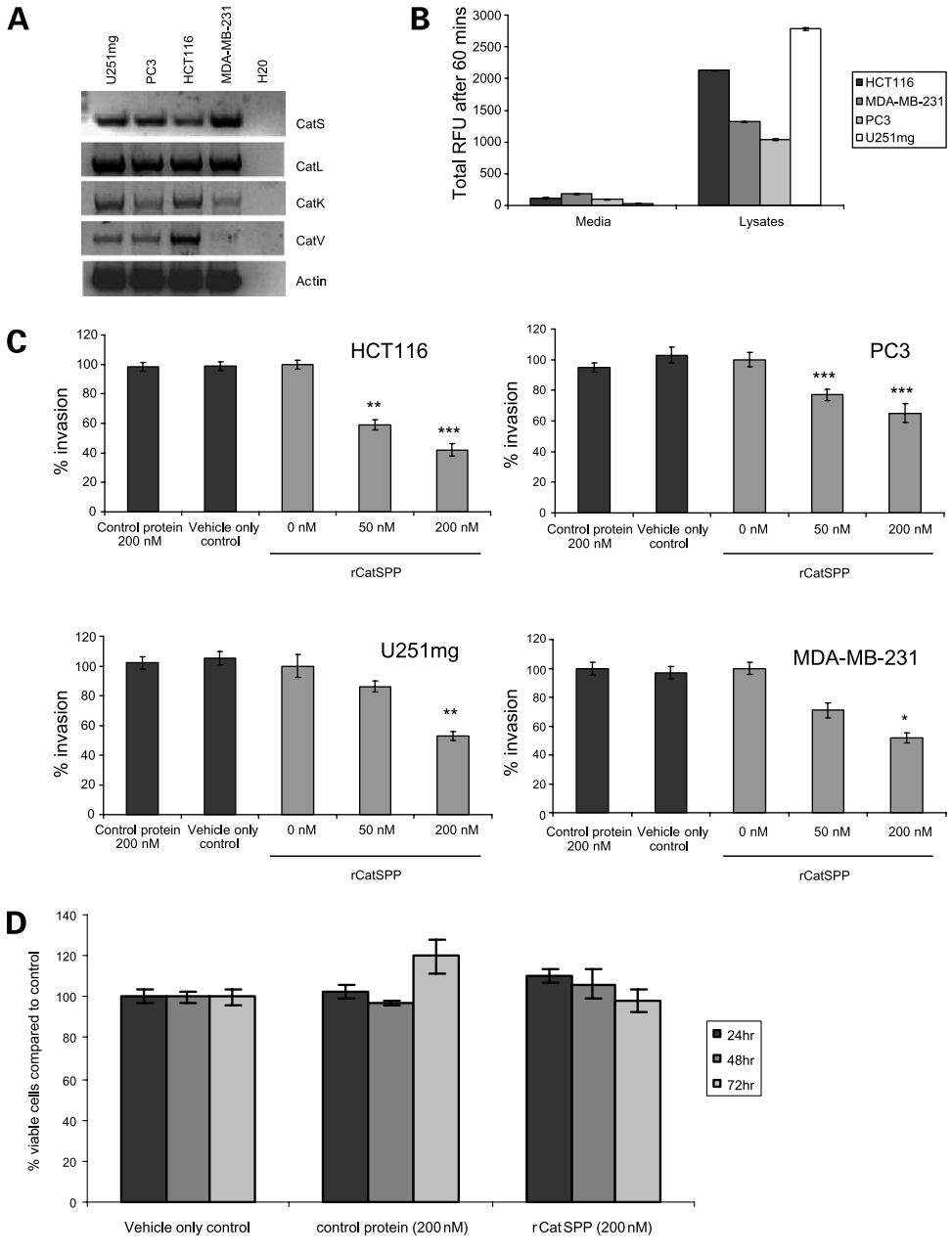

Figure 4. Inhibition of cathepsin L–like proteases in tumor cell lines. The relative expression levels of the cathepsin L–like proteases in HCT116, U251mg, MDA-MB-231, and PC3 human malignant cells lines were examined by reverse transcription-PCR. Amplification of the β-actin was used as an internal control (**A**). The relative activity levels in each of the human tumor cell lines were assessed by fluorimetric assay (**B**). The effect of the rCatSPP on tumor cell invasion was assessed by *in vitro* invasion assays: HCT116, PC3, U251mg, and MDA-MB-231 (**C**). Each of these assays used recombinant NH_2-terminal $(His)_6$-tagged human Lck, expressed, and purified identically as a control. To ensure that the anti-invasive effects observed in the *in vitro* invasion assays were not due to any antiproliferative or cytotoxic effects of the recombinant protein, MTT assay was done on HCT116 cells and incubated with rCatSPP or control protein for 24, 48, and 72 h (**D**).

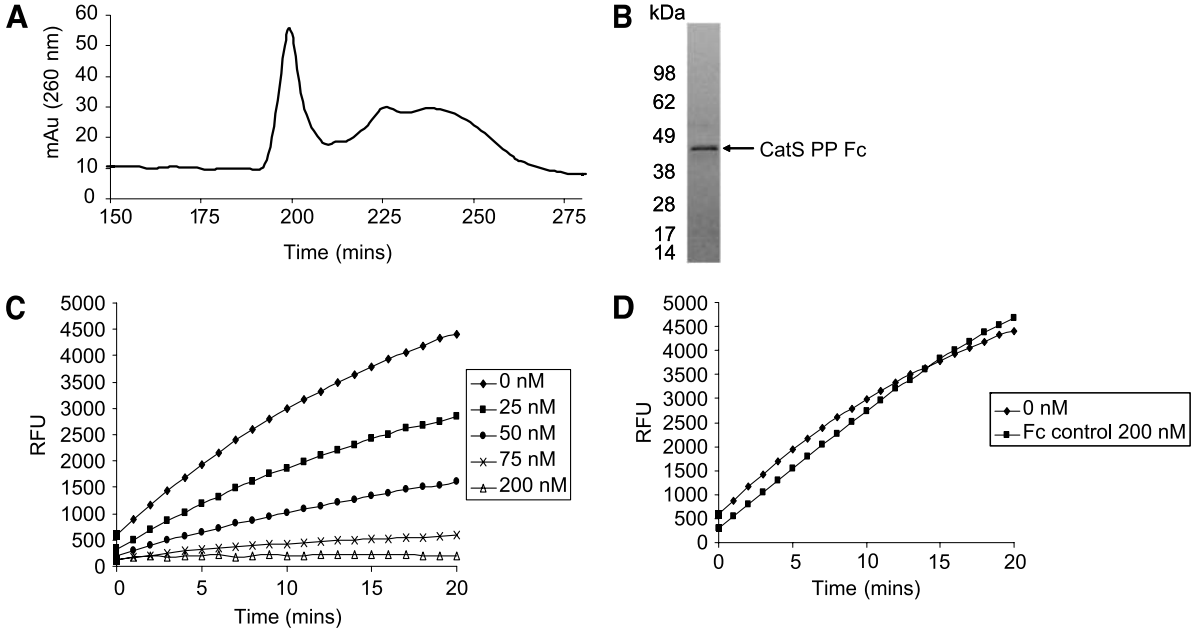

Figure 5. Expression and purification of rCatSPP-Fc. The rCatSPP cDNA sequence was cloned into a modified pRSET bacterial expression vector containing a COOH-terminal IgG Fc-domain. Expression was induced by the addition of IPTG and purification was by virtue of its NH_2-terminal $(His)_6$ tag using IMAC. The purification profile revealed two peaks: analysis of eluted fractions from the second peak by SDS-PAGE revealed the presence of the rCatSPP-Fc at ~46 kDa (**A** and **B**). The biological activity of the rCatSPP-Fc and nonrelated Fc-control protein was ascertained by fluorimetric assay using Cbz-Val-Val-Arg-AMC. The rCatSPP-Fc retained its ability to inhibit the proteolytic activity of cathepsin S (**C**). Analysis of the domain NH_2-terminal $(His)_6$ tag Fc control protein showed that it exhibited no inhibitory activity toward cathepsin S at highest concentrations tested (200 nmol/L; **D**).

via fusion with a COOH-terminal murine IgG_{2b} Fc-domain. Fusion of small therapeutically useful peptides and proteins is useful to stabilize the protein by increasing its half-life, generally as a result of increased size in the resultant fusion protein (22). The recombinant CatSPP-Fc chimera was expressed and purified from bacterial cultures by the NH_2-terminal $(His)_6$ tag using the identical procedure as the original rCatSPP species using a Ni^{2+}-charged IMAC column. The purification profile of the rCatSPP-Fc revealed two main peaks (Fig. 5A) and analysis of the elution fractions from the second peak by SDS-PAGE identified the presence of a highly purified protein species with a molecular weight of ~46 kDa, as expected for the rCatSPP-Fc (Fig. 5B).

Kinetic Evaluation of rCatSPP-Fc toward Cathepsin S

Fluorimetric assays were used to confirm that the rCatSPP-Fc had retained its ability to act as a potent inhibitor of the cathepsin L–like cathepsins and that the COOH-terminal Fc-domain had no negative effects on the kinetics of inhibition. Consequently, rCatSPP-Fc (0-200 nmol/L) was incubated with human cathepsin S in the presence of Cbz-Val-Val-Arg-AMC (25 μmol/L) and the resultant progress curves revealed a dose-dependent inhibition of cathepsin S activity (Fig. 5C). Subsequent Morrison plots revealed that the inhibition constant for the rCatSPP-Fc was reduced ~3.5-fold with an observed K_i of 8.9 ± 2.5 nmol/L in comparison with 2.5 ± 0.12 nmol/L for the original rCatSPP. These effects are probably due to some slight changes in the conformation of the propeptide domain as a result of fusing the Fc-domain onto its COOH terminus. As a control, NH_2-terminally labeled $(His)_6$-tagged Fc-domain protein was expressed, purified, and tested for inhibitory activity using the same fluorimetric assay to confirm that the Fc-domain had no effects on inhibition. It was found that incubation of 200 nmol/L of this control Fc protein with human cathepsin S showed no discernable effects on cathepsin S activity (Fig. 5D).

Inhibition of Tumor Cell Invasion by the rCatSPP-Fc

Having determined that the rCatSPP-Fc could potently inhibit the peptidolytic activity of cathepsin S, albeit at slightly reduced potency, its ability to attenuate tumor cell invasion was investigated in parallel with the original rCatSPP species. Incubation of MDA-MB-231 cells with the rCatSPP (0-250 nmol/L) confirmed the dose-dependent effects observed earlier, with 44% reduction in tumor cell invasion in the presence of 250 nmol/L rCatSPP (Fig. 6A, *top*). However, a significant reduction in tumor cell invasion was observed in the presence of much lower inhibitor concentrations of the rCatSPP-Fc; a 46% reduction in invasion was observed in the presence of only 5 nmol/L of the rCatSPP-Fc, with up to 75% reduction observed in the presence of 50 nmol/L (Fig. 6A, *bottom*).

The relative inhibition/reduction of tumor cell invasion in the presence of the two propeptide species were subjected to nonlinear regression analysis using Prism software, with sigmoidal dose-response curves plotted to

elucidate the relative EC_{50} values for each inhibitor. The rCatSPP was found to have an EC_{50} value of 78.0 nmol/L, whereas the increased potency of the rCatSPP-Fc was clearly evident from the EC_{50} value calculated as 8.3 nmol/L (Fig. 6B).

Finally, to ascertain if the addition of the Fc-domain had enhanced the stability of the protein, resulting in the improvement in EC_{50}, the rCatSPP and the rCatSPP-Fc proteins (500 nmol/L) were incubated with HCT116 cells for 24 h. Conditioned medium was collected and assessed by SDS-PAGE with Western blotting using an anti-polyhistidine tag antibody. The results of these studies are shown in Fig. 6C. The presence of the rCatSPP is clearly evident in the supernatant at the zero time point but cannot be detected beyond this point (Fig. 6C, *top*). In comparison, the stability of the rCatSPP-Fc is clearly enhanced by the addition of the COOH-terminal Fc-domain. The rCatSPP-Fc is clearly present in the zero time point and is still evident after 24 h, although levels appear reduced in a time-dependent manner (Fig. 6C, *bottom*). Finally, whole-cell lysate samples were analyzed by Western blot to see if either propeptide species had been taken up by the cells, but detection of the proteins via their $(His)_6$-tag proved negative (data not shown).

Discussion

Several cysteine cathepsins have been implicated in the invasion and metastatic processes of a range of different malignancies (15, 23, 24). The overexpression and secretion from tumor cells of these proteases frequently correlates with increasing grade of tumor invasiveness (18, 25, 26). Normally, only active at the low pH of activated lysosomes, the cathepsin L–like proteases were originally perceived to have only limited roles in the higher pH of the tumor microenvironment. However, demonstration that at neutral

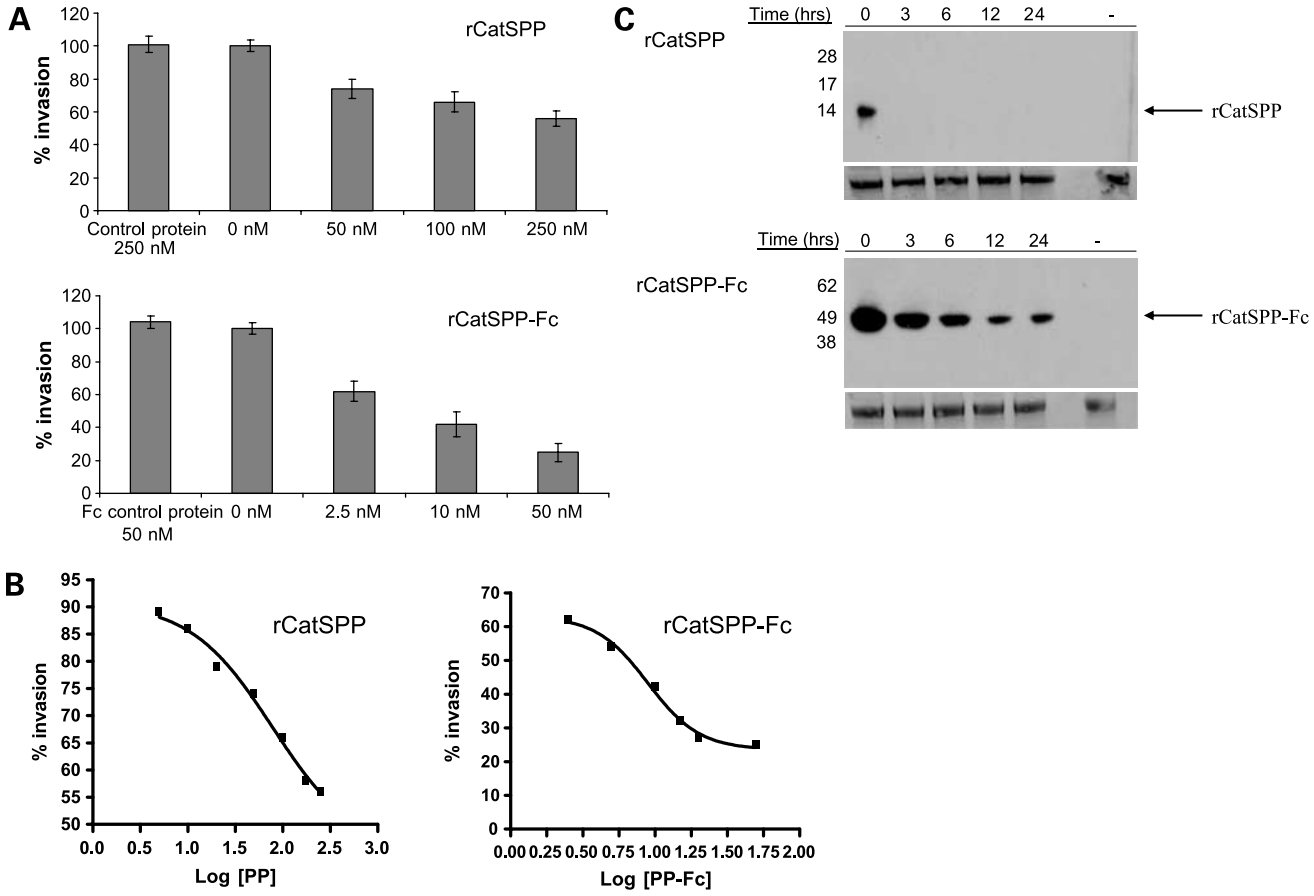

Figure 6. Inhibition of tumor cell invasion by the rCatSPP-Fc. *In vitro* invasion assays comparing the inhibitory effects of the rCatSPP and rCatSPP-Fc were done using MDA-MB-231 cells. Assays were done in the presence of increasing concentrations of the rCatSPP or rCatSPP-Fc (**A**) with appropriate control proteins (human Lck and IgG Fc-domain, respectively). Mean ± SD tumor cell invasion. The relative rate of tumor cell invasion in the presence of varying concentrations of the rCatSPP or rCatSPP-Fc was subjected to nonlinear regression analysis and sigmoidal dose-response curves constructed (**B**). The resultant EC_{50} values were found to be 78.0 and 8.3 nmol/L for the rCatSPP (*i*) and rCatSPP-Fc (*ii*), respectively. Finally, the stability of the rCatSPP and rCatSPP-Fc was determined in the extracellular environment during tissue culture (**C**). The rCatSPP (*top*) and rCatSPP-Fc (*bottom*) proteins were incubated with HCT116 colorectal carcinoma cells to assess the enhanced stability of the recombinant protein due to the addition of the IgG_2 Fc-domain. Samples of supernatant were assessed by SDS-PAGE to determine stability of the proteins and bands were visualized by Western blotting using an anti-$(His)_6$ tag antibody. Membranes were stained with Ponceau red to confirm equal loading of supernatants.

pH cathepsin S can maintain activity (27) and that cathepsin L activity can be stabilized by p41 extracellularly (28) suggest that secreted cathepsin L–like species might play a role in cell invasion. Indeed, a substantial amount of evidence points toward their role in the degradation of elastin, collagen, laminin, and other components of the extracellular matrix (29–33). Furthermore, their role in the coactivation and activation of other proteases, such as the metalloproteases, has also been suggested (34).

Aberrant cathepsin S expression was shown to be significantly greater in astrocytoma and prostate carcinoma sections in comparison with normal tissues (18, 35, 36), whereas cathepsin L overexpression has been identified in a wide range of human malignancies including melanomas, meningiomas, and colorectal carcinomas (37–39). Cathepsin K overexpression has been associated with invasive lung adenocarcinomas (40) and breast carcinomas (41) and also identified as the principal protease in giant cell tumor of the bone (42). Cathepsin V was originally identified in colorectal and breast carcinomas as well as certain ovarian and renal cell carcinomas (24) and is currently one of only two proteases employed in a multigene signature assay to predict recurrence of tamoxifen-treated, node-negative breast carcinomas (43).

Recently, it has been shown that there is involvement of several cysteine cathepsins in tumorigenesis where increases in their expression were observed in a transgenic mouse model of pancreatic carcinoma. Expression of cathepsins L and S and also the more distantly related cathepsins C, H, Z, and B were all increased in the murine angiogenic islets and tumors. Similar effects were also observed in a second mouse model of human cervical carcinogenesis, suggesting that it may be a general phenomenon rather than restricted to particular tumor types (14).

A more comprehensive investigation determining the distinct roles of the cysteine cathepsins in multistage tumorigenesis was done using a RIP1-Tag2 mouse model of pancreatic islet cell carcinogenesis and specific cathepsin-null mice. This study implicated cathepsins B and S in tumor formation and angiogenesis, whereas cathepsins B and L had roles in tumor cell proliferation and tumor growth. Interestingly, the null mutation of cathepsins B, L, or S leads to a perturbation in the progression of the invasive carcinoma, suggesting a possible nonredundant role of each of these proteases (15).

In this study, we have developed a broad-spectrum inhibition strategy to examine the role of cathepsin L–like proteases secreted from tumor cells. The generation of recombinant cathepsin propeptides has been shown previously, where the production of these recombinant proteins resulted in the formation of insoluble inclusion bodies, which necessitated laborious purification and refolding procedures using a GdnHCl concentration gradient (8) or through affinity chromatography and subsequent cleavage using a GST-fusion construct (9). Here, we applied an alternative simplified strategy for the production of the CatSPP recombinant protein using IMAC and on-column refolding, which we have employed previously for the characterization of CatVPP (12). These previous propeptides were kinetically characterized *in vitro*, showing nanomolar inhibitory activities against the cathepsin L–like proteases (9–12), which we have similarly found with the rCatSPP species in this current investigation. Using the specific example of cathepsin S, we showed that the prodomain can block its cleavage of nonfibrillar collagen (gelatin) and elastin in *in vitro* assays, consistent with previous reports that these proteases are involved in the degradation of the extracellular matrix and in agreement that their inhibition will attenuate invasion.

Based on these results, we proceeded to investigate if the rCatSPP could actually be employed in cell-based assays to inhibit the cathepsin L–like proteases in the tumor microenvironment and block cell invasion processes. We observed the significant diminution of cell invasion across a range of cancer cell lines, representative of some of the common forms of tumor, that is, astrocytoma and breast, colorectal, and prostate carcinomas. The propeptide is a small basic polypeptide with limited secondary structure (10) and therefore is likely to have a relatively short half-life in these cell-based invasion assays due to breakdown by other protease species. As anticipated, the fusion of the polypeptide with a COOH-terminal murine IgG Fc-domain significantly improved its half-life and thus its anti-invasive potency. Furthermore, we were unable to detect either prodomain species in whole-cell lysates, showing noninternalization of intact active protein, indicating the effect we were observing was most likely specific to inhibition of extracellular cathepsin L–like activity only.

Our data would suggest that this approach for inhibition of the cathepsin L–like proteases could form the basis of a novel therapeutic strategy to inhibit tumor progression. The synthesis of small-molecule inhibitors for the cathepsin L–like proteases, both reversible and irreversible, has been well documented (44–47). However, the therapeutic application of such compounds is limited by toxicity concerns caused by their possible collateral inhibition of intracellular cathepsin L–like proteases in normal tissues (48). Therefore, alternative strategies that can target only secreted proteolytic activities as observed in pathologies such as malignancy are attractive. Furthermore, inhibitors that have broad specificity against this entire subfamily of proteases may prove more useful due to redundancy in function that has been shown from gene knockout studies (49, 50). Consequently, an appropriate next step will be the evaluation of this fusion protein to attenuate tumor burden and associated tumorigenic processes in *in vivo* studies. Given that this compound is peptide based, its application in animal models such as the RIP1-Tag2 mouse is essential to ensure that efficacious bioavailability and acceptable pharmacokinetics can be achieved.

References

1. Rawlings ND, Tolle DP, Barrett AJ. MEROPS: the peptidase database. Nucleic Acids Res 2004;32:D160–4.

2. Honey K, Rudensky AY. Lysosomal cysteine proteases regulate antigen presentation. Nat Rev Immunol 2003;3:472–82.

3. Bryant P, Ploegh H. Class II MHC peptide loading by the professionals. Curr Opin Immunol 2004;16:96 – 102.

4. Yasuda Y, Kaleta J, Bromme D. The role of cathepsins in osteoporosis and arthritis: rationale for the design of new therapeutics. Adv Drug Deliv Rev 2005;57:973 – 93.

5. Chapman HA, Jr., Munger JS, Shi GP. The role of thiol proteases in tissue injury and remodeling. Am J Respir Crit Care Med 1994;150:S155 – 9.

6. Chapman HA, Riese RJ, Shi GP. Emerging roles for cysteine proteases in human biology. Annu Rev Physiol 1997;59:63 – 88.

7. Mach L, Mort JS, Glossl J. Maturation of human procathepsin B. proenzyme activation and proteolytic processing of the precursor to the mature proteinase, *in vitro*, are primarily unimolecular processes. J Biol Chem 1994;269:13030 – 5.

8. Maubach G, Schilling K, Rommerskirch W, et al. The inhibition of cathepsin S by its propeptide-specificity and mechanism of action. Eur J Biochem 1997;250:745 – 50.

9. Guay J, Falgueyret JP, Ducret A, Percival MD, Mancini JA. Potency and selectivity of inhibition of cathepsin K, L and S by their respective propeptides. Eur J Biochem 2000;267:6311 – 8.

10. Billington CJ, Mason P, Magny MC, Mort JS. The slow-binding inhibition of cathepsin K by its propeptide. Biochem Biophys Res Commun 2000;276:924 – 9.

11. Carmona E, Dufour E, Plouffe C, et al. Potency and selectivity of the cathepsin L propeptide as an inhibitor of cysteine proteases. Biochemistry 1996;35:8149 – 57.

12. Burden RE, Snoddy P, Jefferies CA, Walker B, Scott CJ. Inhibition of cathepsin L – like proteases by cathepsin V propeptide. Biol Chem 2007; 388:541 – 5.

13. Premzl A, Zavasnik-Bergant V, Turk V, Kos J. Intracellular and extracellular cathepsin B facilitate invasion of MCF-10A neoT cells through reconstituted extracellular matrix *in vitro*. Exp Cell Res 2003; 283:206 – 14.

14. Joyce JA, Baruch A, Chehade K, et al. Cathepsin cysteine proteases are effectors of invasive growth and angiogenesis during multistage tumorigenesis. Cancer Cell 2004;5:443 – 53.

15. Gocheva V, Zeng W, Ke D, et al. Distinct roles for cysteine cathepsin genes in multistage tumorigenesis. Genes Dev 2006;20:543 – 56.

16. Koblinski JE, Ahram M, Sloane BF. Unraveling the role of proteases in cancer. Clin Chim Acta 2000;291:113 – 35.

17. Rao JS. Molecular mechanisms of glioma invasiveness: the role of proteases. Nat Rev Cancer 2003;3:489 – 501.

18. Flannery T, Gibson D, Mirakhur M, et al. The clinical significance of cathepsin S expression in human astrocytomas. Am J Pathol 2003;163: 175 – 82.

19. Morrison JF, Walsh CT. The behavior and significance of slow-binding enzyme inhibitors. Adv Enzymol Relat Areas Mol Biol 1988;61:201 – 301.

20. Werle B, Staib A, Julke B, et al. Fluorometric microassays for the determination of cathepsin L and cathepsin S activities in tissue extracts. Biol Chem 1999;380:1109 – 16.

21. Lecaille F, Weidauer E, Juliano MA, Bromme D, Lalmanach G. Probing cathepsin K activity with a selective substrate spanning its active site. Biochem J 2003;375:307 – 12.

22. Zheng XX, Steele AW, Hancock WW, et al. IL-2 receptor-targeted cytolytic IL-2/Fc fusion protein treatment blocks diabetogenic autoimmunity in nonobese diabetic mice. J Immunol 1999;163:4041 – 8.

23. Mohamed MM, Sloane BF. Cysteine cathepsins: multifunctional enzymes in cancer. Nat Rev Cancer 2006;6:764 – 75.

24. Santamaria I, Velasco G, Cazorla M, Fueyo A, Campo E, Lopez-Otin C. Cathepsin L2, a novel human cysteine proteinase produced by breast and colorectal carcinomas. Cancer Res 1998;58:1624 – 30.

25. Sivaparvathi M, Yamamoto M, Nicolson GL, et al. Expression and immunohistochemical localization of cathepsin L during the progression of human gliomas. Clin Exp Metastasis 1996;14:27 – 34.

26. Wang M, Tang J, Liu S, Yoshida D, Teramoto A. Expression of cathepsin B and microvascular density increases with higher grade of astrocytomas. J Neurooncol 2005;71:3 – 7.

27. Kirschke H, Wiederanders B, Bromme D, Rinne A. Cathepsin S from bovine spleen. Purification, distribution, intracellular localization and action on proteins. Biochem J 1989;264:467 – 73.

28. Fiebiger E, Maehr R, Villadangos J, et al. Invariant chain controls the activity of extracellular cathepsin L. J Exp Med 2002;196:1263 – 9.

29. Liu J, Sukhova GK, Sun JS, Xu WH, Libby P, Shi GP. Lysosomal cysteine proteases in atherosclerosis. Arterioscler Thromb Vasc Biol 2004; 24:1359 – 66.

30. Sloane BF, Yan S, Podgorski I, et al. Cathepsin B and tumor proteolysis: contribution of the tumor microenvironment. Semin Cancer Biol 2005;15:149 – 57.

31. Novinec M, Grass RN, Stark WJ, Turk V, Baici A, Lenarcic B. Interaction between human cathepsins K, L, and S and elastins: mechanism of elastinolysis and inhibition by macromolecular inhibitors. J Biol Chem 2007;282:7893 – 902.

32. Wang B, Sun J, Kitamoto S, et al. Cathepsin S controls angiogenesis and tumor growth via matrix-derived angiogenic factors. J Biol Chem 2006;281:6020 – 9.

33. Mai J, Sameni M, Mikkelsen T, Sloane BF. Degradation of extracellular matrix protein tenascin-C by cathepsin B: an interaction involved in the progression of gliomas. Biol Chem 2002;383: 1407 – 13.

34. Kobayashi H, Moniwa N, Sugimura M, Shinohara H, Ohi H, Terao T. Effects of membrane-associated cathepsin B on the activation of receptor-bound prourokinase and subsequent invasion of reconstituted basement membranes. Biochim Biophys Acta 1993;1178:55 – 62.

35. Flannery T, McQuaid S, McGoohan C, et al. Cathepsin S expression: an independent prognostic factor in glioblastoma tumours—a pilot study. Int J Cancer 2006;119:854 – 60.

36. Fernandez PL, Farre X, Nadal A, et al. Expression of cathepsins B and S in the progression of prostate carcinoma. Int J Cancer 2001;95: 51 – 5.

37. Stabuc B, Mrevlje Z, Markovic J, Stabuc-Silih M. Expression and prognostic significance of cathepsin L in early cutaneous malignant melanoma. Neoplasma 2006;53:259 – 62.

38. Trinkaus M, Vranic A, Dolenc VV, Lah TT. Cathepsins B and L and their inhibitors stefin B and cystatin C as markers for malignant progression of benign meningiomas. Int J Biol Markers 2005;20:50 – 9.

39. Troy AM, Sheahan K, Mulcahy HE, Duffy MJ, Hyland JM, O'Donoghue DP. Expression of Cathepsin B and L antigen and activity is associated with early colorectal cancer progression. Eur J Cancer 2004; 40:1610 – 6.

40. Rapa I, Volante M, Cappia S, Rosas R, Scagliotti GV, Papotti M. Cathepsin K is selectively expressed in the stroma of lung adenocarcinoma but not in bronchioloalveolar carcinoma. A useful marker of invasive growth. Am J Clin Pathol 2006;125:847 – 54.

41. Littlewood-Evans AJ, Bilbe G, Bowler WB, et al. The osteoclast-associated protease cathepsin K is expressed in human breast carcinoma. Cancer Res 1997;57:5386 – 90.

42. Lindeman JH, Hanemaaijer R, Mulder A, et al. Cathepsin K is the principal protease in giant cell tumor of bone. Am J Pathol 2004;165: 593 – 600.

43. Paik S, Shak S, Tang G, et al. A multigene assay to predict recurrence of tamoxifen-treated, node-negative breast cancer. N Engl J Med 2004; 351:2817 – 26.

44. Bromme D, Kaleta J. Thiol-dependent cathepsins: pathophysiological implications and recent advances in inhibitor design. Curr Pharm Des 2002;8:1639 – 58.

45. Link JO, Zipfel S. Advances in cathepsin S inhibitor design. Curr Opin Drug Discov Dev 2006;9:471 – 82.

46. Shinozuka T, Shimada K, Matsui S, et al. Potent and selective cathepsin K inhibitors. Bioorg Med Chem 2006;14:6789 – 806.

47. Katunuma N, Matsunaga Y, Himeno K, Hayashi Y. Insights into the roles of cathepsins in antigen processing and presentation revealed by specific inhibitors. Biol Chem 2003;384:883 – 90.

48. Turk V, Kos J, Turk B. Cysteine cathepsins (proteases)—on the main stage of cancer? Cancer Cell 2004;5:409 – 10.

49. Nakagawa T, Roth W, Wong P, et al. Cathepsin L: critical role in degradation and CD4 T cell selection in the thymus. Science 1998;280: 450 – 3.

50. Nakagawa TY, Brissette WH, Lira PD, et al. Impaired invariant chain degradation and antigen presentation and diminished collagen-induced arthritis in cathepsin S null mice. Immunity 1999;10:207 – 17.